

Bounds on the superconducting transition temperature: Applications to twisted bilayer graphene and cold atoms

Tamaghna Hazra,¹ Nishchal Verma,¹ Mohit Randeria^{1*}

¹Department of Physics, The Ohio State University, Columbus, Ohio 43210

(Dated: September 23, 2019)

Understanding the material parameters that control the superconducting transition temperature T_c is a problem of fundamental importance. In many novel superconductors phase fluctuations determine T_c , rather than the collapse of the pairing amplitude. We derive rigorous upper bounds on the superfluid phase stiffness for multi-band systems, valid in any dimension. This in turn leads to an upper bound on T_c in two dimensions (2D), which holds irrespective of pairing mechanism, interaction strength, or order-parameter symmetry. Our bound is particularly useful for the strongly correlated regime of low-density and narrow-band systems, where mean field theory fails. For a simple parabolic band in 2D with Fermi energy E_F , we find that $k_B T_c \leq E_F/8$, an exact result that has direct implications for the 2D BCS-BEC crossover in ultra-cold Fermi gases. Applying our multi-band bound to magic-angle twisted bilayer graphene (MA-TBG), we find that band structure results constrain the maximum T_c to be close to the experimentally observed value. Finally, we discuss the question of deriving rigorous upper bounds on T_c in 3D.

Our work is motivated by the fundamental question: what limits the superconducting (SC) transition temperature T_c ? Within BCS mean-field theory, and its extensions like Eliashberg theory, the amplitude of the SC order parameter is destroyed by the breaking of pairs, and T_c scales with the pairing gap Δ . The material parameters that control the mean-field T_c are the electronic density of states (DOS) at the chemical potential $N(0)$ and the effective interaction, determined by the spectrum of fluctuations that mediate pairing.

Beginning with the pioneering experiments of Uemura [1] and theoretical ideas of Emery and Kivelson [2] on underdoped cuprates, it became clear that the mean field picture of T_c scaling with the pairing gap is simply not valid in many novel superconductors. The loss of SC order is then governed by fluctuations of the phase of the order parameter, rather than the suppression of its amplitude, and T_c is related to the superfluid stiffness D_s . The material parameters that determine D_s are rather different from those that determine the pairing gap Δ .

The question of mean field amplitude collapse versus phase fluctuation dominated SC transition is brought into sharp focus by a variety of recent experiments in narrow band and low density systems. One of the most exciting recent developments is the observation of very narrow bands in magic-angle twisted bilayer graphene (MA-TBG) leading to correlation-induced “Mott” insulating states [3] and superconductivity [4] in their vicinity. Flat bands are also expected to arise in various topological states of matter; see, e.g., [5–8]. BCS theory-based intuition suggests that narrow bands have a large DOS $N(0)$ and lead to high temperature superconductivity. Is this true or do phase fluctuations limit the T_c ?

The extensive compilation of data in Fig. 6 of ref. [4] suggests that all known superconductors have a T_c that scales at most like a constant times the “Fermi energy E_F ”, though there is considerable leeway in defining E_F in strongly correlated and multi-band materials. We also note that ultra-cold Fermi gases in the strongly inter-

acting regime of the BCS-BEC crossover [9, 10] exhibit experimental values [11] of $k_B T_c/E_F$ larger than those observed in the solid state. All of these observations raise the question of ultimate limits on the T_c of a superconductor or paired superfluid.

In this paper, we obtain sharp answers to these questions, especially in 2D. First, we derive an upper bound on the superfluid stiffness $D_s(T) \leq \tilde{D}(T)$, where \tilde{D} is proportional to the optical conductivity sum rule. This inequality is valid in all dimensions and for arbitrary interactions. We then use the Berezinskii-Kosterlitz-Thouless (BKT) theory in 2D to obtain $k_B T_c \leq \pi \tilde{D}(T_c)/2$.

While the bound on T_c is of completely general validity, it is most useful in the strongly correlated regime of narrow-band and low density systems, precisely where conventional mean-field approaches fails. We show that \tilde{D} is necessarily “small” in such systems, and, in many cases of interest, \tilde{D} is essentially determined by the (non-interacting) band structure.

We give several examples that illustrate the usefulness of our bounds for a variety of systems. For a single parabolic band we show that $k_B T_c \leq E_F/8$ in 2D. This exact result poses stringent constraints on the T_c of the 2D BCS-BEC crossover in ultra cold atoms. We also describe bounds on T_c for the 2D attractive Hubbard model, relevant for current optical lattice experiments [12], that demonstrate the tension between breaking of pairs and phase fluctuations, and highlight the connection with a pairing pseudogap [13, 14].

Turning to multi-band systems, we use available band structure results [15–19] for MA-TBG to calculate \tilde{D} and thus constrain its T_c without any assumptions about the pairing mechanism or order-parameter symmetry. We obtain a rigorous (but weak) bound of $\simeq 15$ K. Using physically motivated approximations, we estimate a bound on T_c as low as 6 K.

Finally, we discuss the question of deriving similar bounds in 3D. We show that the presence of non-universal

pre-factors in the relation between T_c and D_s , as well their scaling behavior near a SC quantum critical point, pose challenges in deriving a rigorous bound in 3D.

Results: We first outline our main results and then give a detailed derivation and specific applications. We consider a Fermi system described by the general Hamiltonian

$$\mathcal{H} = \mathcal{H}_K + \mathcal{H}_{\text{int}}; \quad \mathcal{H}_K = \sum_{\mathbf{k}, m, \sigma} \epsilon_m(\mathbf{k}) c_{\mathbf{k}m\sigma}^\dagger c_{\mathbf{k}m\sigma} \quad (1)$$

where \mathbf{k} is crystal momentum, m is a band label, and σ the spin. \mathcal{H}_K is the kinetic energy and \mathcal{H}_{int} describes interactions (electron-phonon, electron-electron, etc.), including those that give rise to superconductivity. The external vector potential \mathbf{A} enters \mathcal{H} through a Peierl's substitution in the tight-binding representation of \mathcal{H}_K , but does not affect \mathcal{H}_{int} . For now, we ignore disorder and return to it at the end.

The macroscopic superfluid stiffness D_s determines the free energy cost of distorting the phase of the SC order parameter $|\Delta|e^{i\theta}$ via the Boltzmann factor $\exp(-D_s \int d^d \mathbf{r} |\nabla \theta|^2 / 2k_B T)$. It is related to the London penetration depth via $1/\lambda_L^2 = (4\mu_0 e^2 / \hbar^2) D_s$ in 3D. Microscopically, D_s can be calculated as the static, long wavelength limit of the transverse current response [20, 21] to a vector potential. (Our results are equally valid for neutral superfluids with rotation playing the role of the magnetic field.) We obtain a rigorous upper bound valid in any dimension

$$D_s(T) \leq \tilde{D}(T) = \frac{\hbar^2}{4\Omega} \sum_{\mathbf{k}, mm', \sigma} M_{mm'}^{-1}(\mathbf{k}) \langle c_{\mathbf{k}m\sigma}^\dagger c_{\mathbf{k}m'\sigma} \rangle \quad (2)$$

where Ω is the volume of the system and $M_{mm'}^{-1}(\mathbf{k})$ is an inverse mass tensor that depends only on the electronic structure of \mathcal{H}_K ; see eq. (5) below. The temperature and interactions impact \tilde{D} only through $\langle c_{\mathbf{k}m\sigma}^\dagger c_{\mathbf{k}m'\sigma} \rangle$, where the thermal average is calculated using the full \mathcal{H} .

We next use D_s to provide an upper bound on the SC transition temperature in 2D. We use the Nelson-Kosterlitz [22] universal relation to obtain

$$k_B T_c \leq \pi \tilde{D}(T_c) / 2 \quad (3)$$

For a weak coupling superconductor, T_c is well described by mean field theory and our result, though valid as an upper bound, may not be very useful. On the other hand, as we show below, for a strongly interacting system the bound gives insight into both the value of T_c and on its dependence on parameters.

Bound on superfluid stiffness: The intuitive idea behind $D_s \leq \tilde{D}$ is as follows. $(2\pi e^2 / \hbar^2) \tilde{D} = \int_0^\infty d\omega \text{Re } \sigma(\omega)$ is the optical conductivity spectral weight integrated over the bands in eq. (1), and $(4\pi e^2 / \hbar^2) D_s$ is the coefficient of the $\delta(\omega)$ piece in $\text{Re } \sigma(\omega)$ in the SC state; (note: $\int_0^\infty d\omega \delta(\omega) = 1/2$). The inequality (2) says that the weight in the SC delta-function must be less than or equal to the total spectral weight.

To derive (2), we use the Kubo formula for D_s as a linear response [20, 21] to an external vector potential in an arbitrary direction a

$$D_s = \tilde{D} - (\hbar^2 / 4e^2) \chi_{ja,ja}^\perp(\mathbf{q} \rightarrow 0, \omega = 0), \quad (4)$$

where \tilde{D} is the diamagnetic response $\sim \langle \delta^2 \mathcal{H} / \delta A_a^2 \rangle$, while χ^\perp is the *transverse* current-current correlation function. \tilde{D} is given by eq. (2) with

$$M_{mm'}^{-1}(\mathbf{k}) = \sum_{\alpha\beta} U_{m,\alpha}^\dagger(\mathbf{k}) \frac{\partial^2 t_{\alpha\beta}(\mathbf{k})}{\partial (\hbar k_a)^2} U_{\beta,m'}(\mathbf{k}) \quad (5)$$

Here α, β label orbitals/sites within a unit cell of a Bravais lattice, $t_{\alpha\beta}(\mathbf{k})$ is the Fourier transform of the hopping $t_{\alpha\beta}(\mathbf{r}_{i\alpha} - \mathbf{r}_{j\beta})$, and $U_{\alpha,m}(\mathbf{k})$ is the unitary transformation that diagonalizes $t_{\alpha\beta}(\mathbf{k})$ to the band basis $\epsilon_m(\mathbf{k})\delta_{m,m'}$. The inverse mass tensor in eq. (5) also depends on the direction $a = x, y, \dots$ through the derivative with respect to k_a on the right hand side, however, we do not show this a dependence explicitly to simplify the notation. These results are derived in Appendix A, and the relation to the optical sum rule shown in Appendix B; see also ref. [23].

We next turn to the second term in eq. (4). From its Lehmann representation we see that $\chi^\perp(\mathbf{q} \rightarrow 0, \omega = 0) \geq 0$ at all temperatures; see Appendix C. We thus obtain $D_s(T) \leq \tilde{D}(T)$.

For a single band system eqs. (2) and (5) simplify greatly and we get $\tilde{D} = (4\Omega)^{-1} \sum_{\mathbf{k}, \sigma} (\partial^2 \epsilon(\mathbf{k}) / \partial k_a^2) n_\sigma(\mathbf{k})$, where the momentum distribution $n_\sigma(\mathbf{k}) = \langle c_{\mathbf{k}\sigma}^\dagger c_{\mathbf{k}\sigma} \rangle$. This allows us to recover well-known special cases. (1) With nearest neighbor (NN) hopping on a square or cubic lattice, $\partial^2 \epsilon(\mathbf{k}) / \partial k_a^2 \sim \epsilon(\mathbf{k})$, and \tilde{D} is proportional to the kinetic energy. (2) A parabolic dispersion $\epsilon(\mathbf{k}) = \hbar^2 k^2 / 2m$ leads to the simple result $\tilde{D} = \hbar^2 n / 4m$, independent of T and of interactions. Here $D_s(T) = \hbar^2 n_s(T) / 4m$ and our bound simply says that the superfluid density $n_s(T) \leq n$ the total density.

For materials with non-parabolic dispersion and/or multiple bands, \tilde{D} depends on T and interactions. It is thus illuminating to derive a bound for \tilde{D} which depends only on the density. We describe the single band result here, relegating the multi-band generalization to Appendix D. We write $\mathcal{H}_K = - \sum_{\mathbf{R}\delta\sigma} [t(\delta) c_{\mathbf{R}+\delta,\sigma}^\dagger c_{\mathbf{R},\sigma} + \text{h.c.}]$ with translationally invariant hopping amplitudes $t(\delta)$ that depend only the vector δ connecting lattice sites \mathbf{R} and $\mathbf{R} + \delta$. We couple the system to a vector potential and compute \tilde{D} , which involves terms like $\sum_{i,j} \delta_a^2 t(\delta) \langle c_i^\dagger c_j \rangle$ with $\delta = i - j$ (schematically). We note that $\tilde{D} \geq 0$, since it is the sum rule for $\text{Re } \sigma(\omega) \geq 0$. We then use the triangle inequality and Cauchy-Schwarz $|\langle c_i^\dagger c_j \rangle| \leq \sqrt{\langle n_i \rangle \langle n_j \rangle} = n$ to obtain $D_s \leq \tilde{D} \leq n \sum_{\delta} \delta_a^2 |t(\delta)| / 2$. This shows that for small hopping and/or low density, one necessarily has a small D_s .

T_c bound in 2D: For a BKT transition in 2D, the T_c and the stiffness D_s are related by the universal ratio [22] $k_B T_c / D_s(T_c^-) = \pi/2$. Together with eq. (2) $D_s(T_c^-) \leq \tilde{D}(T_c)$, we then immediately obtain eq. (3). In an anisotropic system \tilde{D} depends on $a = x, y$ through the $\partial^2 / \partial k_a^2$ in eq. (5). We can use $\tilde{D} = \max\{\tilde{D}_x, \tilde{D}_y\}$ to obtain a bound on T_c , however, we argue in Appendix H, for a much stronger result $\tilde{D} = [\tilde{D}_x \tilde{D}_y]^{1/2}$ in 2D.

We emphasize that eq. (3) with $\tilde{D}(T_c)$ on the RHS is sufficient to derive the rigorous results below. However, to obtain the intuitively more appealing result $k_B T_c \leq \pi \tilde{D}(0)/2$, we need to assume that $D_s(T)$ is a decreasing function of T , so that $D_s(T_c^-) \leq D_s(0) \leq \tilde{D}(0)$.

2D Parabolic Dispersion: Consider a single band with $\epsilon(\mathbf{k}) = \hbar^2 k^2 / 2m$ with density n , so that the Fermi energy $E_F = \pi \hbar^2 n / m$ and arbitrary interactions that lead to pairing and superconductivity. Then $M^{-1}(\mathbf{k}) = m^{-1}$ and $\Omega^{-1} \sum_{\mathbf{k}, \sigma} \tilde{n}_\sigma(\mathbf{k}; T) = n$ independent of T and interactions, so that $\tilde{D} = \hbar^2 n / 4m$. Eq. (3) then leads to the simple result

$$k_B T_c \leq E_F / 8 \quad (6)$$

which must be obeyed independent of the strength of attraction or order-parameter symmetry, provided the system exhibits a BKT transition. In a weak-coupling superconductor T_c will actually be *much smaller* than $E_F/8$ but, as we discuss next, the bound can be saturated in systems with strong interactions, such as the 2D BCS-BEC crossover experiments in ultra-cold Fermi gases.

2D BCS-BEC crossover: In ultra-cold Fermi gas experiments the two-body s-wave interaction between atoms is tuned using a Feshbach resonance. This has led to deep insights into the crossover [9, 10] from the weak coupling BCS limit with large Cooper pairs all the way to the BEC of tightly bound diatomic molecules. Asymptotically exact results are available in both the BCS and BEC limits, however, the crossover regime between the two extremes is very strongly interacting, with pair size comparable to the inter-particle spacing, and is much less understood. It is precisely here that our exact upper bound (6) is relevant.

The 2D crossover for s-wave pairing is parameterized by the dimensionless interaction [24] $\log(E_b/E_F)$, where E_b is the binding energy of the two-body bound state in vacuum and E_F the Fermi energy. In the weak-coupling BCS limit ($E_b \ll E_F$), the mean field $k_B T_c \sim \sqrt{E_F E_b}$ [24], with a pre-factor that has been computed including the Gorkov-Melik-Barkhudarov (GMB) correction [25, 26]. Clearly T_c is much smaller than our bound.

In the BEC limit ($E_b \gg E_F$) the composite bosons have mass $2m$, density $n/2$, and an inter-boson scattering length a_b where $E_b/E_F \sim 1/na_b^2$ [26]. The 2D dilute Bose gas has $k_B T_c = E_F/[2 \log \log(2/na_b^2)]$ [27], which is valid in the regime $\log \log \gg 1$. This too is smaller

than our bound, though our exact result cautions against a naive extrapolation of the BEC limit result into the strong interaction regime.

The results of the 2D Fermi gas experiment of ref. [28] seems to violate eq. (6) in the crossover regime. We note, however, that our bound is obtained for a strictly 2D system in the thermodynamic limit, while the experiment is on a quasi-2D system in a harmonic trap, from which it is difficult to accurately determine the BKT T_c . The finite size of the trap raises T_c ; even the non-interacting Bose gas in a 2D harmonic trap has a non-zero T_c .

Magic angle twisted bilayer graphene: Let us next turn to a multi-band system of great current interest. The existence of very narrow bands in MATBG was predicted by continuum electronic structure calculations [15, 16] that pointed out the crucial role of $\alpha = w/\hbar v_F^0 K \theta$, where θ is the twist angle between the two layers, w is the interlayer tunneling, v_F^0 the bare Fermi velocity, and K the Dirac-node location in monolayer graphene. It was predicted that v_F in TBG can be tuned to zero [15], with a bandwidth less than 10 meV by choosing certain magic angles θ , the largest of which $\approx 1.1^\circ$ has now been achieved in experiments [3, 4]. Recently, pressure-tuning of w has also resulted in very narrow bands [29].

Little is known at this time about the nature of the SC state or the pairing mechanism, though the observed non-linear I-V characteristics [3, 4] are consistent with a BKT transition. Proximity to a ‘‘Mott’’ insulator and narrow bandwidth suggest the importance of electron correlations, while the extreme sensitivity of the dispersion to structure suggests that electron-phonon interactions could also be important. We argue here that simply using the available electronic structure information for MATBG, and without any prejudice about the interactions responsible for SC, we can put strong constraints on its superconducting T_c .

There are two bands for each of the two valleys, one above and the other below the charge neutrality point (CNP). Each band has a two-fold spin degeneracy, with bands for one valley related to those of the other by time-reversal. We include these eight bands in the $\sum_{mm', \sigma}$ in eq. (2), while the $\sum_{\mathbf{k}}$ is over the moiré Brillouin zone, a hexagon with side $2K \sin(\theta/2) \simeq K\theta$. We use the tight-binding model of ref. [17], a multi-parameter fit to the continuum dispersion [15], to calculate $M_{m, m'}^{-1}(\mathbf{k})$ of eq. (5), which is block-diagonal in the valley index, so that there are no cross-valley terms in eq. (2).

To derive a general bound, where we make no simplifying assumptions, we start with $\tilde{D} \geq 0$ and obtain $\tilde{D} \leq (\hbar^2/4\Omega) \sum_{\mathbf{k}mm', \sigma} |M_{mm'}^{-1}(\mathbf{k})| |\langle c_{\mathbf{k}m\sigma}^\dagger c_{\mathbf{k}m'\sigma} \rangle|$ using the triangle inequality. We next use Cauchy-Schwarz to obtain $|\langle c_{\mathbf{k}m\sigma}^\dagger c_{\mathbf{k}m'\sigma} \rangle|^2 \leq n_{m\sigma}(\mathbf{k}) n_{m'\sigma}(\mathbf{k}) \leq 1$, since the momentum distribution $n_{m\sigma}(\mathbf{k}) \leq 1$. We thus find $\tilde{D} \leq (\hbar^2/4\Omega) \sum_{\mathbf{k}, m, m', \sigma} |M_{mm'}^{-1}(\mathbf{k})|$ which leads to the bound $k_B T_c \leq 56$ K.

We can obtain a more stringent T_c bound if we fur-

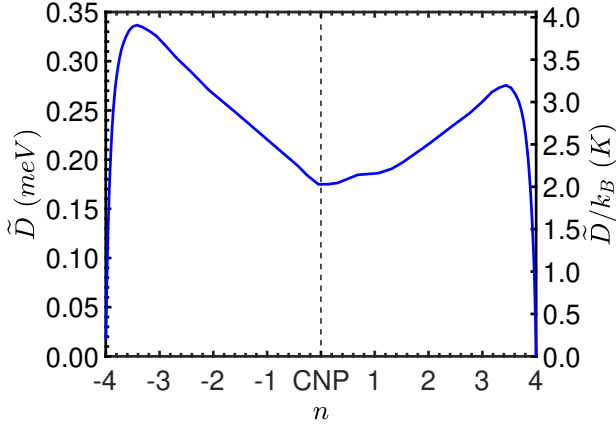


FIG. 1. \tilde{D} as a function of doping from the charge neutrality point (CNP) in magic angle-twisted bilayer graphene (MA-TBG), calculated using the band structure of ref. [17] at $T=0$. $(2\pi e^2/\hbar^2)\tilde{D}$ is the integrated optical spectral weight and $\pi\tilde{D}/2$ is an upper bound on the SC T_c in MA-TBG.

ther physical inputs. The “Mott” gap in the correlated insulator is experimentally [3, 4] known to be ≈ 0.3 meV, and we expect a superconducting gap which is at most that value. Thus we may assume that, at half-filling away from CNP on the hole doped side, say, the bands above the CNP are essentially empty and unaffected by pairing.

Before proceeding, we derive a general result valid for arbitrary interactions which shows that inter-band terms do not contribute to eq. (2) for completely filled or empty bands. To prove this, we again use the Cauchy-Schwarz inequality $|\langle c_{\mathbf{k}m\sigma}^\dagger c_{\mathbf{k}m'\sigma} \rangle|^2 \leq n_{m\sigma}(\mathbf{k})n_{m'\sigma}(\mathbf{k}) = 0$ when either band m or m' is empty. A similar argument works for the filled case after a particle-hole transformation; see Appendix E. Thus $\langle c_{\mathbf{k}m\sigma}^\dagger c_{\mathbf{k}m'\sigma} \rangle = 0$ for $m \neq m'$, whenever either of the two bands is completely filled or empty, and only $m=m'$ terms survive in eq. (2).

To bound T_c for MA-TBG near half-filling on the *hole-doped side* of the CNP, we take $n_m(\mathbf{k})=0$ for the empty bands above the CNP, as explained above. Keeping only band-diagonal terms and using the triangle inequality we obtain $\tilde{D} \leq (\hbar^2/4\Omega) \sum_{\mathbf{k},m,\sigma} |M_{mm}^{-1}(\mathbf{k})| n_{m\sigma}(\mathbf{k})$. Using $n(\mathbf{k}) \leq 1$ for the bands below CNP we obtain the bound $T_c \leq 14.4$ K near half-filling for hole doping using the tight-binding model of ref. [17]. A similar calculation leads to $T_c \leq 15.0$ K near half-filling for electron doping; see Appendix F. We note that using $|M^{-1}|$ and general constraints on $n(\mathbf{k})$ leads to rigorous results, but weakens the bounds.

Finally, we make a physically motivated estimate of \tilde{D} , which yields an improved, but approximate, result. We use the $T=0$ band theory result $\langle c_{\mathbf{k}m\sigma}^\dagger c_{\mathbf{k}m'\sigma} \rangle = \delta_{m,m'} \Theta(\mu - \epsilon_m(\mathbf{k}))$, with the chemical potential μ determined by the density $\Omega^{-1} \sum_{\mathbf{k},m,\sigma} n_{m\sigma}(\mathbf{k})$. This, together with $M_{mm}^{-1}(\mathbf{k})$ calculated from the tight binding model of ref. [17], leads to the density-dependent estimate of \tilde{D} plotted in Fig. 1. We note that using $\partial^2/\partial k_x^2$

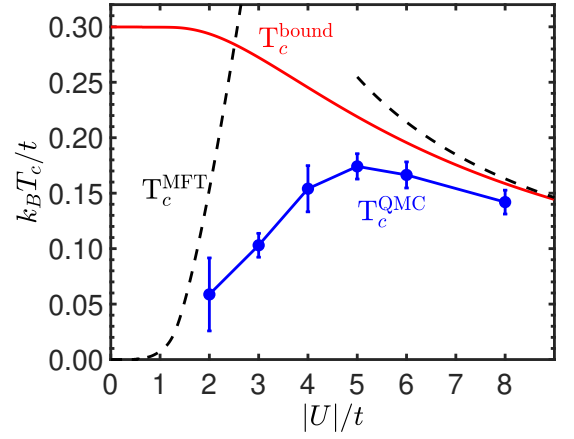


FIG. 2. T_c for the 2D attractive Hubbard model at density $n = 0.7$ with QMC results from ref. [30]. The BCS mean field T_c^{MFT} controls T_c at weak coupling. Phase fluctuations, estimated using our upper bound T_c^{bound} (see text) dominate at intermediate and strong coupling, where we also show the $t^2/|U|$ asymptotics of our bound.

versus $\partial^2/\partial k_y^2$ to calculate M^{-1} affects our estimates by less than a percent.

The integrated optical spectral weight, given by $(2\pi e^2/\hbar^2)\tilde{D}$, vanishes at the band insulators when all bands are either filled or empty. Clearly our band-structure based estimate does not know about the “Mott” insulating states at half-filling away from CNP. $(\pi/2)$ times the \tilde{D} plotted in Fig. 1 is an estimated upper bound on the SC T_c . The system is not SC over most of the doping range, but our bound is the maximum attainable T_c if the system were to exhibit superconductivity. We find the maximum T_c to be about 6 K, while the experimental value is 3 K [29].

We note that the T_c bounds are sensitive to the precise electronic structure results we use as input for calculating M^{-1} . As shown in Appendix F, using the tight binding results of ref. [18] for MA-TBG, leads to a T_c estimate about 2.5 times higher than the one presented above, based on the band structure of ref. [17]. We emphasize that these differences arise from the fact that the details of the non-interacting band structure of MA-TBG are not very well established. Irrespective of that, our results suggest that MA-TBG is a strongly correlated SC in a phase fluctuation dominated regime.

2D attractive Hubbard model and optical lattices: We next obtain important insights on the value of T_c and its interaction-dependence for the 2D attractive Hubbard model, where we can compare our bound with sign problem free Quantum Monte Carlo (QMC) simulations [30]. This system has also been investigated in recent optical lattice experiments [12].

Consider nearest-neighbor (NN) hopping on a square lattice with $\mathcal{H} = -t \sum_{\langle i,j \rangle \sigma} c_{i,\sigma}^\dagger c_{j,\sigma} + \text{h.c.} - |U| \sum_i (n_{i\uparrow} - 1/2)(n_{i\downarrow} - 1/2)$. For $n \neq 1$ the system has an s-wave SC ground state, exhibiting a crossover from

a weak coupling BCS state ($|U|/t \ll 1$) to a BEC of hard-core on-site bosons ($|U|/t \gg 1$). The QMC estimate [30] of T_c , obtained from the BKT jump in the D_s , is a non-monotonic function of $|U|/t$ at a fixed density n ; see Fig. 2. The BCS mean field T_c^{MFT} correctly describes the weak coupling T_c , (For a more accurate estimate, one should take into account the GMB correction [25] which suppresses the numerical pre-factor, but does not alter the functional form of T_c^{MFT} .) For $|U|/t > 2$, T_c^{MFT} is the scale at which pairs dissociate and lies well above T_c . In the $|U|/t \gg 1$ limit we see $T_c \sim t^2/|U|$, the effective boson hopping.

Our bound permits us to understand $T_c(|U|/t)$ in the intermediate coupling regime where there are no other reliable analytical estimates. To estimate \tilde{D} analytically, we need to make an approximation for $n(\mathbf{k})$. If we choose a step-function (as we did for the MA-TBG) we get $T_c \leq 0.3t$ for $n=0.7$, independent of $|U|/t$.

To obtain a better estimate, we note that, as $|U|/t$ increases, the pair-size shrinks and $n(\mathbf{k})$ broadens. In the extreme $|U|/t$ -limit of on-site bosons, $n(\mathbf{k})$ is flat (\mathbf{k} -independent), leading to $\tilde{D} \rightarrow 0$, since $\partial^2 \epsilon / \partial k_x^2$ is a periodic function with zero mean whose \mathbf{k} -sum vanishes. To model this broadening of $n(\mathbf{k})$, we use the results of the $T=0$ BCS-Leggett crossover theory; see Appendix G. This gives us the (approximate) bound plotted in Fig. 2, which has the correct $t^2/|U|$ asymptotic behavior at large $|U|$.

In general, we see that $T_c \leq \min \{T_c^{\text{MFT}}, \pi \tilde{D} / 2k_B\}$. For temperatures between the pairing scale T_c^{MFT} and T_c at which phase coherence sets in, the “normal state” exhibits a pseudogap due to pre-formed pairs [13, 14].

Three dimensional systems: Experiments suggest that there may be an upper bound on T_c in 3D systems; see, e.g., Fig. 6 of ref. [4]. We have not succeeded in deriving a rigorous bound on the 3D T_c , unlike in 2D. There are two challenges that one faces in trying to derive a bound in 3D, one related to rigorous control on numerical pre-factors and the other to the functional form of the relation between T_c and D_s . Both are related to the fact that in 3D the superfluid stiffness does not have dimensions of energy, unlike in 2D.

Following Emery and Kivelson (EK) [2], we focus on the 3D phase ordering temperature $k_B T_\theta = A D_s(0) \bar{a}$, which could provide a bound on T_c . Here A is a (dimensionless) constant and \bar{a} is the length-scale up to which one has to coarse-grain to derive an effective XY model. EK use $\bar{a}^2 = \pi \xi^2$, where ξ is the coherence length, and suggest, based on Monte Carlo results for classical XY models, that $A \simeq 4.4$ gave a reasonable account of experiments on underdoped cuprates and other materials.

However, the coefficient A is *non-universal* and can vary from one system to another. Consider the 3D problem of the BCS-BEC crossover in ultra-cold Fermi gases [10] with $\hbar^2 k^2 / 2m$ dispersion and interaction, characterized by the s-wave scattering length a_s , tuned using a Feshbach resonance. At unitarity ($|a_s| = \infty$),

the experimental $k_B T_c \simeq 0.17 E_F$ [11], while QMC estimates [31, 32] range from $k_B T_c \simeq 0.15 E_F - 0.17 E_F$. QMC shows the expected non-monotonic behavior of $k_B T_c / E_F$ as a function of $1/k_F a_s$, with a maximum $k_B T_c / E_F \simeq 0.22$ at a small positive $1/k_F a_s$. The maximum value of $k_B T_c / E_F$ is *larger* than the non-interacting BEC result, consistent with the rigorous result [33] that repulsive interactions increase the T_c of a dilute Bose gas in 3D.

We choose $\xi \simeq k_F^{-1}$ near unitarity [34] and try to use $k_B T_\theta = A(\hbar^2 n / 4m)(\sqrt{\pi} \xi)$ as a bound on T_c . Consistency with the observed $k_B T_c / E_F \simeq 0.22$ then requires $A \simeq 7.4$, quite different from the 4.4 quoted above. We do not know if there is a definite value of A that would give a “phase-ordering” upper bound on T_c in 3D.

The following argument suggests that there may, in fact, be no *general* bound on T_c that is linear in $D_s(0)$ in 3D. From a practical point of view, one is interested in learning about the highest T_c in a class of materials. But, if a general bound were to exist, it should be equally valid in situations where both T_c and $D_s(0)$ are driven to zero by tuning a (dimensionless) parameter $\delta \rightarrow 0^+$ toward a quantum critical point (QCP). From the action $S = \frac{1}{2} D_s \int_0^\beta d\tau \int d^d \mathbf{r} |\nabla \theta|^2 + \dots$ describing the phase fluctuations of the SC order parameter, we get the quantum Josephson scaling relation [35] $D_s(0) \sim \delta^{(z+d-2)\nu}$. One also obtains, as usual, $T_c \sim \delta^{z\nu}$, where z and ν are the dynamical and correlation length exponents in d spatial dimensions. Thus $T_c \sim [D_s(0)]^{z/(z+d-2)}$ near the QCP. In 2D, this gives a linear scaling between T_c and $D_s(0)$. However, in 3D we get $T_c \sim D_s(0)^{z/(z+1)}$ which, sufficiently close to the QCP, will necessarily violate an upper bound on T_c that is conjectured to scale linearly with $D_s(0)$. This is not just an academic issue, as experiments see precisely such a deviation from linear scaling with $T_c \sim \sqrt{D_s(0)}$, consistent with $z = 1$, both in highly underdoped [36, 37] and in highly overdoped [38, 39] cuprates.

Concluding remarks: We have thus far ignored disorder. We note that D_s of the pure system is necessarily larger than that in the disordered system. This can be seen by generalizing Leggett’s bound [40] on the superfluid density (derived in the context of supersolids) to the case of disordered systems [41]. Thus our upper bounds for translationally invariant systems continue to be valid in the presence of disorder, although they can be improved.

Although we have focused on narrow band and low density systems here, our bounds have also important implications for systems close to insulating states, either correlation-driven or disorder-driven. In either case, if there is a continuous superconductor to insulator transition, the superfluid stiffness will eventually become smaller than the energy gap and control the SC T_c .

As a design principle, it is interesting to ask if one can have multi-band systems where a narrow band has a large energy gap and large “mean field” T_c interacting with a broad band that makes a large contribution to the

superfluid stiffness, thus getting the best of both worlds.

Acknowledgments We are grateful to P. Törmä, S. Peotta and L. Liang for pointing out an error in an earlier version of our paper that led us to the correct multi-band

result presented here. We thank J. Kang and O. Vafek for providing the tight-binding parameters for ref. [18]. We acknowledge support from NSF DMR-1410364 and the Center for Emergent Materials, an NSF MRSEC, under Award Number DMR-1420451.

-
- [1] Y. J. Uemura *et. al.*, *Physical Review Letters* **62**, 2317 (1989).
 - [2] V. J. Emery and S. A. Kivelson, *Nature* **374**, 434 (1995).
 - [3] Y. Cao, V. Fatemi, A. Demir, S. Fang, S. L. Tomarken, J. Y. Luo, J. D. Sanchez-Yamagishi, K. Watanabe, T. Taniguchi, E. Kaxiras, R. C. Ashoori, and P. Jarillo-Herrero, *Nature* **556**, 80 (2018).
 - [4] Y. Cao, V. Fatemi, S. Fang, K. Watanabe, T. Taniguchi, E. Kaxiras, and P. Jarillo-Herrero, *Nature* **556**, 43 (2018).
 - [5] N. B. Kopnin, T. T. Heikkilä, and G. E. Volovik, *Physical Review B* **83**, 220503 (2011).
 - [6] E. Tang and L. Fu, *Nature Physics* **10**, 964 (2014).
 - [7] S. Peotta and P. Törmä, *Nature Communications* **6**, 8944 (2015).
 - [8] L. Liang, T. I. Vanhala, S. Peotta, T. Siro, A. Harju, and P. Törmä, *Physical Review B* **95**, 024515 (2017).
 - [9] W. Ketterle and M. W. Zwierlein, in *Ultracold Fermi Gases, Proc. of the Int. Sch. of Phys. “Enrico Fermi, Course CLXIV, Varenna, 2006*, edited by M. Inguscio, W. Ketterle, and C. Salomon (IOS Press, Amsterdam, 2008).
 - [10] M. Randeria and E. Taylor, *Annual Review of Condensed Matter Physics* **5**, 209 (2014).
 - [11] M. J. H. Ku, A. T. Sommer, L. W. Cheuk, and M. W. Zwierlein, *Science* **335**, 563 (2012).
 - [12] D. Mitra, P. Brown, E. Guardado-Sanchez, S. S. Kondov, T. Devakul, D. A. Huse, P. Schauss, and W. Bakr, *Nature Physics* **14**, 173 (2018).
 - [13] M. Randeria, N. Trivedi, A. Moreo, and R. T. Scalettar, *Physical Review Letters* **69**, 2001 (1992).
 - [14] N. Trivedi and M. Randeria, *Physical Review Letters* **75**, 312 (1995).
 - [15] R. Bistritzer and A. H. MacDonald, *Proceedings of the National Academy of Sciences* **108**, 12233 (2011).
 - [16] J. M. B. Lopes dos Santos, N. M. R. Peres, and A. H. Castro Neto, *Physical Review Letters* **99**, 256802 (2007).
 - [17] M. Koshino, N. F. Q. Yuan, T. Koretsune, M. Ochi, K. Kuroki, and L. Fu, *Physical Review X* **8**, 031087 (2018).
 - [18] J. Kang and O. Vafek, *Physical Review X* **8**, 031088 (2018).
 - [19] H. C. Po, L. Zou, A. Vishwanath, and T. Senthil, *Physical Review X* **8**, 031089 (2018).
 - [20] G. Baym, in *Mathematical Methods in Solid State and Superfluid Theory*, edited by R. C. Clark and G. H. Derrick (Springer US, 1968).
 - [21] D. J. Scalapino, S. R. White, and S. Zhang, *Physical Review B* **47**, 7995 (1993).
 - [22] D. R. Nelson and J. M. Kosterlitz, *Physical Review Letters* **39**, 1201 (1977).
 - [23] B. Valenzuela, M. J. Calderón, G. León, and E. Bascones, *Physical Review B* **87**, 075136 (2013).
 - [24] M. Randeria, J.-M. Duan, and L.-Y. Shieh, *Physical Review Letters* **62**, 981 (1989).
 - [25] L. P. Gor’kov and T. Melik-Barkhudarov, *Zh. Eksp. Teor. Fiz.* **40**, 1452 (1961), [*Sov. Phys. JETP*, **13** 1018 (1961)].
 - [26] D. S. Petrov, M. A. Baranov, and G. V. Shlyapnikov, *Physical Review A* **67**, 031601 (2003).
 - [27] D. S. Fisher and P. C. Hohenberg, *Physical Review B* **37**, 4936 (1988).
 - [28] M. G. Ries, A. N. Wenz, G. Zürn, L. Bayha, I. Boettcher, D. Kedar, P. A. Murthy, M. Neidig, T. Lompe, and S. Jochim, *Physical Review Letters* **114**, 230401 (2015).
 - [29] M. Yankowitz, S. Chen, H. Polshyn, Y. Zhang, K. Watanabe, T. Taniguchi, D. Graf, A. F. Young, and C. R. Dean, *Science* **363**, 1059 (2019).
 - [30] T. Paiva, R. Scalettar, M. Randeria, and N. Trivedi, *Physical Review Letters* **104**, 066406 (2010).
 - [31] E. Burovski, E. Kozik, N. Prokof’ev, B. Svistunov, and M. Troyer, *Physical Review Letters* **101**, 090402 (2008).
 - [32] O. Goulko and M. Wingate, *Physical Review A* **82**, 053621 (2010).
 - [33] R. Seiringer and D. Ueltschi, *Physical Review B* **80**, 014502 (2009).
 - [34] J. R. Engelbrecht, M. Randeria, and C. A. R. Sáde Melo, *Physical Review B* **55**, 15153 (1997).
 - [35] M. P. A. Fisher, P. B. Weichman, G. Grinstein, and D. S. Fisher, *Physical Review B* **40**, 546 (1989).
 - [36] I. Hetel, T. R. Lemberger, and M. Randeria, *Nature Physics* **3**, 700 (2007).
 - [37] D. M. Broun, W. A. Huttema, P. J. Turner, S. Özcan, B. Morgan, R. Liang, W. N. Hardy, and D. A. Bonn, *Physical Review Letters* **99**, 237003 (2007).
 - [38] T. R. Lemberger, I. Hetel, A. Tsukada, M. Naito, and M. Randeria, *Physical Review B* **83**, 140507 (2011).
 - [39] I. Božović, X. He, J. Wu, and A. T. Bollinger, *Nature* **536**, 309 (2016).
 - [40] A. J. Leggett, *Phys. Rev. Lett.* **25**, 1543 (1970).
 - [41] A. Paramekanti, N. Trivedi, and M. Randeria, *Physical Review B* **57**, 11639 (1998).

Appendix A: Linear response, D_s and \tilde{D}

Let us consider the general Hamiltonian

$$\mathcal{H} = \mathcal{H}_K + \mathcal{H}_{\text{int}} \quad (\text{A1})$$

where \mathcal{H}_{int} represents arbitrary interactions, including those that gives rise to superconductivity, and \mathcal{H}_K is the most general single particle Hamiltonian for a multi-band/multi-orbital lattice model

$$\mathcal{H}_K = \sum_{i\alpha j\beta\sigma} t_{\alpha\beta}(\mathbf{r}_{i\alpha} - \mathbf{r}_{j\beta}) c_{i\alpha}^\dagger c_{j\beta}. \quad (\text{A2})$$

Here $t_{\alpha\beta}(\mathbf{r}_{i\alpha} - \mathbf{r}_{j\beta})$ represents the hopping matrix element from orbital β in unit cell j to orbital α in unit cell i with i, j spanning all unit cells, including $i = j$. *We omit the spin label σ only to simplify notation but we are not ignoring spin*, as emphasized by the spin sum. In the presence of an external vector potential \mathbf{A} , the hopping picks up the Peierls phase

$$\mathcal{H}_K \rightarrow \mathcal{H}_K = \sum_{\mathbf{R}, \alpha\beta\sigma} t_{\alpha\beta}(\mathbf{r}) e^{-ie\mathbf{A}(\mathbf{R}) \cdot \mathbf{r}/\hbar} c_{i\alpha}^\dagger c_{j\beta} \quad (\text{A3})$$

where we use the notation $\mathbf{R} = (\mathbf{r}_{i\alpha} + \mathbf{r}_{j\beta})/2$ and $\mathbf{r} = \mathbf{r}_{i\alpha} - \mathbf{r}_{j\beta}$ for simplicity. Since we are eventually interested in the long wavelength limit $\mathbf{q} \rightarrow 0$, we choose a very slowly varying vector potential and write $\int_{\mathbf{r}_{j\beta}}^{\mathbf{r}_{i\alpha}} \mathbf{A} \cdot d\mathbf{l} \simeq \mathbf{A}(\mathbf{R}) \cdot \mathbf{r}$.

Within linear response theory we can Taylor expand the exponential retaining terms which are linear (paramagnetic) and quadratic (diamagnetic) in \mathbf{A} . We transform to Fourier space using $t_{\alpha\beta}(\mathbf{k}) = \sum_{\mathbf{r}} t_{\alpha\beta}(\mathbf{r}) e^{-i\mathbf{k} \cdot \mathbf{r}}$ and $c_{i\alpha} = \Omega^{-1/2} \sum_{\mathbf{k}} e^{i\mathbf{k} \cdot \mathbf{r}_{i\alpha}} d_{\mathbf{k}\alpha}$. We can then write the current operator $j_x = \delta\mathcal{H}_K/\delta A_x$ as the sum of the paramagnetic (P) and diamagnetic (D) current operators given by

$$j_x^P(\mathbf{q}) = \frac{e}{\hbar\Omega} \sum_{\alpha\beta, \mathbf{k}\sigma} \frac{\partial t_{\alpha\beta}(\mathbf{k})}{\partial k_x} d_{\mathbf{k}+\mathbf{q}/2, \alpha}^\dagger d_{\mathbf{k}-\mathbf{q}/2, \beta} \quad (\text{A4})$$

$$j_x^D(\mathbf{q}) = \frac{e^2}{\hbar^2\Omega} \sum_{\alpha\beta, \mathbf{k}\sigma} \frac{\partial^2 t_{\alpha\beta}(\mathbf{k})}{\partial k_x^2} d_{\mathbf{k}\alpha}^\dagger d_{\mathbf{k}\beta} A_x(\mathbf{q}), \quad (\text{A5})$$

where we only show the x -component for simplicity. Note that the paramagnetic current operator, when transformed to the band basis, will in general have interband matrix elements [7, 8]. The only property of $j_x^P(\mathbf{q})$ that we will need to use below, however, is that it is a Hermitian operator; see equation (C1).

The superfluid stiffness D_s is defined as the static long-wavelength limit of the transverse response of the current density \mathbf{j} to a vector potential \mathbf{A}

$$\langle j_x \rangle(\mathbf{q}, \omega) = \frac{-4e^2}{\hbar^2} D_s A_x(\mathbf{q}, \omega) \quad \text{with } q_x = 0, q_\perp \rightarrow 0, \omega = 0 \quad (\text{A6})$$

and \perp represents the orthogonal directions to x . Standard linear response theory leads to the Kubo formula

$$D_s = \tilde{D} - \frac{\hbar^2}{4e^2} \chi_{j_x j_x}^\perp(\mathbf{q} \rightarrow 0, \omega = 0) \quad (\text{A7})$$

where the first term is the diamagnetic term, which is of central interest in this work, and the second is the transverse paramagnetic current-current correlation function. We will focus on the latter in Appendix C, where we show that $\chi_{j_x j_x}^\perp \geq 0$ at all temperatures.

Here we focus on the first term that can be read off from the form of the diamagnetic current operator. We find it convenient to write it in the band basis as

$$\tilde{D} = \frac{\hbar^2}{4\Omega} \sum_{mm', \mathbf{k}\sigma} M_{mm'}^{-1}(\mathbf{k}) \langle c_{\mathbf{k}m}^\dagger c_{\mathbf{k}m'} \rangle \quad (\text{A8})$$

with the inverse mass tensor given by

$$M_{mm'}^{-1}(\mathbf{k}) = \sum_{\alpha\beta} U_{m, \alpha}^\dagger(\mathbf{k}) \frac{\partial^2 t_{\alpha\beta}(\mathbf{k})}{\partial (\hbar k_x)^2} U_{\beta, m'}(\mathbf{k}). \quad (\text{A9})$$

The unitary transformation U that transforms from the orbital to the band basis is defined by

$$\sum_{\alpha\beta} U_{m, \alpha}^\dagger(\mathbf{k}) t_{\alpha\beta}(\mathbf{k}) U_{\beta, m'}(\mathbf{k}) = \epsilon_m(\mathbf{k}) \delta_{m, m'}. \quad (\text{A10})$$

This allows us to write the final result in the band basis using

$$d_{\mathbf{k}\alpha} = \sum_m U_{\alpha, m}(\mathbf{k}) c_{\mathbf{k}m}. \quad (\text{A11})$$

We note several important points about the inverse mass tensor $M_{mm'}^{-1}(\mathbf{k})$. (i) It depends only on the bare band structure, and is independent of temperature and interactions, (ii) it has both diagonal and off-diagonal terms in the band indices. and (iii) it is *not* simply related to the curvature of the bands $\partial^2 \epsilon_m(\mathbf{k})/\partial k_x^2$, in contrast to the single-band case in equation (A12).

The standard reference on the formalism for calculating the superfluid stiffness in lattice systems is Scalapino, White and Zhang (SWZ) [21]. Our normalization conventions differ from them and, more importantly, they focus on the special case of a single band model with nearest-neighbor (NN) hopping on a square (or cubic) lattice. Thus it may be useful for us to provide a “dictionary” relating our results to theirs.

In the single-band case our expression for \tilde{D} reduces to

$$\tilde{D} = \frac{1}{4\Omega} \sum_{\mathbf{k}\sigma} \frac{\partial^2 \epsilon(\mathbf{k})}{\partial k_x^2} n(\mathbf{k}) \quad (\text{A12})$$

where the momentum distribution

$$n(\mathbf{k}) = \langle c_{\mathbf{k}}^\dagger c_{\mathbf{k}} \rangle. \quad (\text{A13})$$

This result is valid for arbitrary one-band dispersion. For the special case of nearest-neighbor (NN) hopping on a square (or cubic) lattice, it is easy to see that the right hand side of equation (A12) is proportional to the kinetic energy in the x -direction, $\langle -K_x \rangle$ in the notation of SWZ. Our result thus reduces to

$$\tilde{D} \rightarrow \langle -K_x \rangle / 4. \quad (\text{A14})$$

Finally, we note that our superfluid stiffness D_s is related to that of SWZ by

$$D_s = (\hbar^2 / 4\pi e^2) D_s^{\text{SWZ}} \quad (\text{A15})$$

Appendix B: Relation between \tilde{D} and optical spectral weight

To see that \tilde{D} is proportional to the optical sum rule spectral weight, we identify the dynamical conductivity $\sigma(\omega)$ as the current response to an electric field $\mathbf{E} = -\partial_t \mathbf{A}$

$$i\omega \sigma(\omega) = \left[\chi_{j_x j_x}(\mathbf{q} = 0, \omega) - \frac{4e^2}{\hbar^2} \tilde{D} \right] \quad (\text{B1})$$

Using the Kramers-Krönig relation

$$\omega \text{Im} \sigma(\omega) = -\frac{2}{\pi} \text{P} \int_0^\infty d\omega' \text{Re} \sigma(\omega') \frac{\omega^2}{\omega'^2 - \omega^2} \quad (\text{B2})$$

and $\text{Re} \chi_{j_x j_x}(\omega \rightarrow \infty) \rightarrow 0$, we obtain the sum rule for the optical conductivity as

$$\int_0^\infty d\omega \text{Re} \sigma(\omega) = \frac{2\pi e^2}{\hbar^2} \tilde{D} \quad (\text{B3})$$

Appendix C: Derivation of Bound $D_s \leq \tilde{D}$

We show that $\chi_{j_x j_x}(\mathbf{q}, \omega = 0) \geq 0$ at any temperature. This follows directly from its Lehmann representation

$$\frac{1}{Z} \sum_{ij} \left[\frac{e^{-\beta E_i} - e^{-\beta E_j}}{E_j - E_i} \right] |\langle i | j_x^P(\mathbf{q}) | j \rangle|^2 \geq 0 \quad (\text{C1})$$

where $|i\rangle$ and $|j\rangle$ are exact eigenstates of the full Hamiltonian \mathcal{H} in equation (A1) with eigenvalues E_i, E_j and $Z = \text{Tr}[e^{-\beta \mathcal{H}}]$. The last inequality follows from $(e^{-x} - e^{-y})/(y - x) \geq 0$. At zero temperature, this expression reduces to

$$\chi_{j_x j_x}(\mathbf{q}, \omega = 0) = 2 \sum_i \frac{|\langle i | j_x^P(\mathbf{q}) | 0 \rangle|^2}{E_i - E_0} \geq 0 \quad (\text{C2})$$

where $|0\rangle$ is the ground state. From equation (A7), we thus conclude that

$$D_s \leq \tilde{D} \quad (\text{C3})$$

Appendix D: Real space bound on \tilde{D}

Except in the case of a single parabolic band, \tilde{D} depends in general on both the T and the interactions, since the thermal average in $\langle c_{\mathbf{k}\mathbf{m}}^\dagger c_{\mathbf{k}\mathbf{m}'} \rangle$ is calculated using the full \mathcal{H} . It is thus illuminating to derive an upper bound for \tilde{D} which shows that \tilde{D} must become small when the densities are low or if all the hopping parameters are small. Such a bound for the single-band case with arbitrary dispersion was sketched in the paper. Here we turn to the multi band case.

It is convenient to start with the real space representation

$$\tilde{D} = \frac{1}{4\Omega} \sum_{\mathbf{R}\mathbf{r}, \alpha\beta\sigma} r_x^2 t_{\alpha\beta}(\mathbf{r}) \langle c_{i\alpha}^\dagger c_{j\beta} \rangle. \quad (\text{D1})$$

Here both forward and backward hopping are accounted for in $\sum_{\mathbf{r}}$ with $t_{\alpha\beta}(|\mathbf{r}|) = t_{\beta\alpha}^*(|\mathbf{r}|)$. Since $\tilde{D} \geq 0$ we can use the triangle inequality. Further using the Cauchy-Schwarz inequality we get

$$\begin{aligned} \tilde{D} &\leq \frac{1}{4\Omega} \sum_{\mathbf{R}\mathbf{r}, \alpha\beta\sigma} r_x^2 |t_{\alpha\beta}(\mathbf{r})| \langle c_{i\alpha}^\dagger c_{j\beta} \rangle \\ &\leq \frac{1}{4\Omega} \sum_{\mathbf{R}\mathbf{r}, \alpha\beta\sigma} r_x^2 |t_{\alpha\beta}(\mathbf{r})| \sqrt{n_{i\alpha} n_{j\beta}} \end{aligned} \quad (\text{D2})$$

where $n_{i\alpha} = \langle c_{i\alpha}^\dagger c_{i\alpha} \rangle$.

Here and below we define an inner product for operators A, B in terms of the thermal expectation value $\langle A^\dagger B \rangle$, which allows us to use the Cauchy-Schwarz inequality $|\langle A^\dagger B \rangle|^2 \leq \langle A^\dagger A \rangle \langle B^\dagger B \rangle$.

Appendix E: Interband contributions to \tilde{D}

We discuss here the conditions under which we can ignore the inter-band contributions to \tilde{D} given by

$$\tilde{D} = \frac{\hbar^2}{4\Omega} \sum_{mm', \mathbf{k}\sigma} M_{mm'}^{-1}(\mathbf{k}) \langle c_{\mathbf{k}\mathbf{m}}^\dagger c_{\mathbf{k}\mathbf{m}'} \rangle \quad (\text{E1})$$

This requires us to understand when $\langle c_{\mathbf{k}\mathbf{m}}^\dagger c_{\mathbf{k}\mathbf{m}'} \rangle = 0$ for $m \neq m'$. We show here that this is the case, *independent of interactions*, when (a) either one of the two bands is empty, and (b) when either one of the two bands is fully filled.

We use the Cauchy-Schwarz inequality (see end of Appendix D) to obtain

$$|\langle c_{\mathbf{k}\mathbf{m}}^\dagger c_{\mathbf{k}\mathbf{m}'} \rangle| \leq \sqrt{n_m(\mathbf{k}) n_{m'}(\mathbf{k})} \quad (\text{E2})$$

where $n_m(\mathbf{k}) = \langle c_{\mathbf{k}\mathbf{m}}^\dagger c_{\mathbf{k}\mathbf{m}} \rangle$ is the momentum distribution function, and equality holds for $m = m'$. For $m \neq m'$, if either band is completely empty, $n_m(\mathbf{k}) = 0$ for all \mathbf{k}

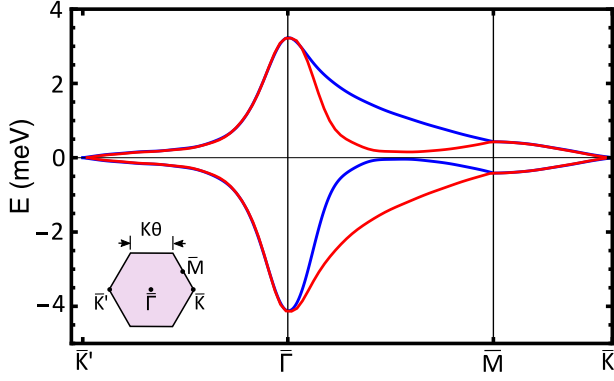


FIG. 3. Energy dispersion for MA-TBG along high-symmetry lines in the moire Brillouin zone (BZ) for the continuum model dispersion [15] that is accurately described by the tight-binding model of Koshino *et. al.* [17]. The bands shown in red and blue correspond to the two valleys of the original BZ and are related by time reversal.

and the inter-band contribution to \tilde{D} in equation (E1) vanishes.

A similar argument for completely filled bands follows from a particle-hole transformation $c_{m\mathbf{k}} \rightarrow h_{m\mathbf{k}}^\dagger$. Since $\langle c_{m\mathbf{k}}^\dagger c_{m'\mathbf{k}'} \rangle = -\langle h_{m\mathbf{k}}^\dagger h_{m'\mathbf{k}'} \rangle$,

$$\begin{aligned} \left| \langle c_{m\mathbf{k}}^\dagger c_{m'\mathbf{k}'} \rangle \right| &= \left| \langle h_{m\mathbf{k}}^\dagger h_{m'\mathbf{k}'} \rangle \right| \\ &\leq \sqrt{n_m^h(\mathbf{k}) n_{m'}^h(\mathbf{k}')} \\ &= \sqrt{(1 - n_m(\mathbf{k})) (1 - n_{m'}(\mathbf{k}'))}. \end{aligned} \quad (\text{E3})$$

Thus we conclude that for filled and empty bands, the inter-band terms do not contribute to the sum in equation (E1), even in the presence of arbitrary interactions.

Finally, we note the simple fact that within band theory there are no inter-band contributions to \tilde{D} . In the absence of interactions (denoted by subscript 0) we obtain

$$\langle c_{m\mathbf{k}}^\dagger c_{m'\mathbf{k}'} \rangle_0 = f(\epsilon_m(\mathbf{k})) \delta_{m,m'} \quad (\text{E4})$$

where f is the Fermi function.

Appendix F: Magic Angle Twisted Bilayer Graphene (MA-TBG)

Magic angles in twisted bilayer graphene were first predicted by the continuum model [15]. Following up on the experimental discovery of correlation-induced insulators and superconductivity in MA-TBG, there has been considerable progress in understanding its electronic structure [17–19]. We first focus on the bounds that we obtain from the tight binding model of Koshino *et. al.* [17], and then at the end of the Appendix compare these with the results we obtain from the tight binding model of Kang and Vafeek [18].

The continuum model dispersion [15] is accurately reproduced by the multi-parameter tight binding fit of Koshino *et. al.* [17] (see Fig. 3) which takes into account hopping over distances up to $9|\mathbf{L}_M|$ where \mathbf{L}_M is the moire lattice vector. We use the hopping integrals presented in the Supplementary Information file `eff_hopping_ver2.dat` of ref. [17] to construct the non-interacting Hamiltonian \mathcal{H}_K of equation (A2). We then identify the unitary matrix $U(\mathbf{k})$ that diagonalizes $t_{\alpha\beta}(\mathbf{k})$ (see equation (A10)) and use it together with $t_{\alpha\beta}(\mathbf{k})$ to compute the inverse mass tensor

$$M_{mm',a}^{-1}(\mathbf{k}) = \sum_{\alpha\beta} U_{m,\alpha}^\dagger(\mathbf{k}) \frac{\partial^2 t_{\alpha\beta}(\mathbf{k})}{\partial(\hbar k_a)^2} U_{\beta,m'}(\mathbf{k}). \quad (\text{F1})$$

Note that we have made explicit here the direction $a = x, y$ as an additional subscript on M^{-1} .

The inverse mass tensor, obtained from the band structure information as described above, is used to compute \tilde{D}_x and \tilde{D}_y and bound T_c as described in the paper. The additional input needed to determine \tilde{D} using equation (A8) is $\langle c_{m\mathbf{k}}^\dagger c_{m'\mathbf{k}'} \rangle$, and we took two different approaches to compute this.

In the first approach, we looked at SC near half-filling on the hole-doped side of the CNP, and argued that the chemical potential was sufficiently far from the CNP that we can take the band above the CNP to be empty. Then using the result of Appendix E we can ignore all inter-band terms with $m \neq m'$. For the occupied band we only used the general constraint that $n(\mathbf{k}) \leq 1$. Using the triangle inequality, we then obtain

$$\tilde{D}_a \leq \frac{\hbar^2}{4\Omega} \sum_{\mathbf{k}, m, \sigma} |M_{mm,a}^{-1}(\mathbf{k})|. \quad (\text{F2})$$

where the empty bands above the CNP are excluded from the sum.

A similar reasoning also works for SC in the vicinity of half-filling on the electron-doped side of the CNP, where we need to use the fact that the bands below CNP are filled to eliminate inter-band terms following Appendix E. We use a particle hole transformation $c_{m\mathbf{k}} \rightarrow h_{m\mathbf{k}}^\dagger$, under which $t_{\alpha\beta}(\mathbf{k}) \rightarrow -t_{\alpha\beta}(\mathbf{k})$ and thus $M^{-1} \rightarrow -M^{-1}$. We write \tilde{D} in terms of the hole momentum distribution functions $n_m^h(\mathbf{k}) = \langle h_{m\mathbf{k}}^\dagger h_{m\mathbf{k}} \rangle$ to get

$$\tilde{D}_a = \frac{\hbar^2}{4\Omega} \sum_{m, \mathbf{k}, \sigma} M_{mm,a}^{-1}(\mathbf{k}) (n_m^h(\mathbf{k}) - 1). \quad (\text{F3})$$

We then show that the second term on the right hand side vanishes as follows:

$$\begin{aligned} \sum_{m, \mathbf{k}} M_{mm,a}^{-1}(\mathbf{k}) &= \sum_{\mathbf{k}, \alpha\beta} \frac{\partial^2 t_{\alpha\beta}(\mathbf{k})}{\partial(\hbar k_a)^2} \sum_m U_{m,\alpha}^\dagger(\mathbf{k}) U_{\beta,m}(\mathbf{k}) \\ &= \sum_{\mathbf{k}, \alpha} \frac{\partial^2 t_{\alpha\alpha}(\mathbf{k})}{\partial(\hbar k_a)^2} = 0. \end{aligned} \quad (\text{F4})$$

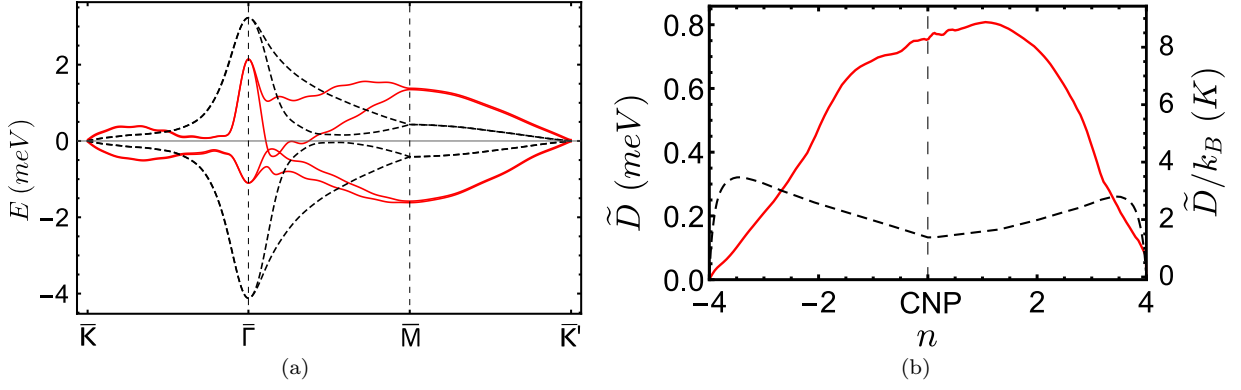


FIG. 4. Comparison of (a) the band structure and (b) the integrated spectral weight \tilde{D} for the models in ref. [17] (in black) and ref. [18] (in red).

We have first used $\sum_m U_{\beta,m}(\mathbf{k})U_{m,\alpha}^\dagger(\mathbf{k}) = \delta_{\beta,\alpha}$, which follows from the unitarity of U , and then the fact that $\partial^2 t_{\alpha\alpha}(\mathbf{k})/\partial k_a^2$ is a periodic function with zero mean, whose $\sum_{\mathbf{k}}$ vanishes. Using the triangle inequality and the general constraint $n^h(\mathbf{k}) \leq 1$, we obtain an expression for electron doping which is similar to the hole-doped case:

$$\tilde{D}_a \leq \frac{\hbar^2}{4\Omega} \sum_{\mathbf{k}m,\sigma} |M_{mm,a}^{-1}(\mathbf{k})| \quad (\text{F5})$$

where now the filled bands below the CNP are excluded from the sum. These bounds, though rigorous, are weak because they involve $|M^{-1}|$ and only very general constraints on $n(\mathbf{k})$.

The second (approximate) approach was to simply use a $T = 0$ (non-interacting) band-theory estimate. We thus use equation (E4) to obtain

$$\tilde{D}_a \simeq \frac{\hbar^2}{4\Omega} \sum_{\mathbf{k}m,\sigma} M_{mm,a}^{-1}(\mathbf{k}) \Theta(\mu - \epsilon_m(\mathbf{k})) \quad (\text{F6})$$

with the chemical potential μ determined by the density. We found that \tilde{D}_x and \tilde{D}_y calculated from the tight binding model of ref. [17] differ by less than a percent. The resulting density-dependent \tilde{D} is shown in Fig. 1 of the main paper.

We note that there are many different tight binding models for describing the narrow bands in MA-TBG and our T_c bounds depend on this input. We have focused above on the results based on ref. [17] with an electronic structure that has separate charge conservation at the K and K' valleys. A rather different model without valley-charge conservation was derived [18] using only time-reversal and point group symmetry. We compare in Fig. 4(a) the band structures of ref. [17] in black and that of ref. [18] in red. The corresponding integrated spectral weights \tilde{D} are shown in Fig. 4(b) using the same color convention. The maximum T_c based on the band structure of ref. [18] is 15 K, which is 2.5 times larger than that estimated from ref. [17].

Appendix G: Attractive Hubbard Model

It is interesting to ask how our bound on SC T_c in 2D depends on interactions. We use the attractive Hubbard model on a square lattice as a concrete example to understand these trends, and to compare our bound with estimates of T_c from sign-problem free quantum Monte Carlo simulations.

Our bound is $k_B T_c \leq \pi/(8\Omega) \sum_{\mathbf{k},\sigma} (\partial_{k_x}^2 \epsilon(\mathbf{k})) n_\sigma(\mathbf{k})$. This result can be written in terms of the kinetic energy $\langle -K_x \rangle$ as discussed at the end of Appendix A. The interaction-dependence is contained in the momentum distribution function $n_\sigma(\mathbf{k})$ which, as we argued in the paper, must become increasingly broader and flatter as $|U|/t$ increases. In the weak coupling BCS limit (small $|U|/t$) $n_\sigma(\mathbf{k})$ is almost like the Fermi function at $T = 0$, very slightly broadened by the superconductivity. On the other hand in the extreme BEC limit (large $|U|/t$) of nearly on-site bosons, the $n_\sigma(\mathbf{k})$ of the constituent fermions is essentially flat.

We model this $|U|/t$ trend in the momentum distribution using the BCS-Leggett crossover theory expression

$$n_\sigma(\mathbf{k}) = \frac{1}{2} \left(1 - \frac{\epsilon(\mathbf{k}) - \mu}{E(\mathbf{k})} \right) \quad (\text{G1})$$

where $E(\mathbf{k}) = \sqrt{(\epsilon(\mathbf{k}) - \mu)^2 + \Delta^2}$ is the Bogoliubov quasiparticle energy. The chemical potential μ and the pair potential Δ are determined self-consistently for a given density n and attraction $|U|$ by solving the $T = 0$ gap and number equations

$$\frac{1}{|U|} = \frac{1}{\Omega} \sum_{\mathbf{k},\sigma} \frac{1}{2E(\mathbf{k})} \quad (\text{G2})$$

$$n = \frac{1}{\Omega} \sum_{\mathbf{k},\sigma} n_\sigma(\mathbf{k}) \quad (\text{G3})$$

We see from Fig. 2 that the T_c obtained from QMC data [30] is always lower than T_c^{bound} . Fig. 2 also shows that the bound is most useful in the intermediate to

strong coupling regime, and less useful in the weak coupling regime where T_c is, in fact, well described by T_c^{MFT} , the pair breaking energy scale.

Appendix H: T_c Bounds in spatially anisotropic systems

We collect here some results on the role of spatial anisotropy focusing mainly on 2D. We note that various quantities that we have considered are different in different directions labeled by $a = x, y$. We have shown that

$$D_{s,a}(T) \leq \tilde{D}_a(T). \quad (\text{H1})$$

The most conservative bound on T_c in 2D is then

$$k_B T_c \leq \frac{\pi}{2} \max \left\{ \tilde{D}_x, \tilde{D}_y \right\}. \quad (\text{H2})$$

Clearly this bound is not optimal because we expect T_c to go to zero if either $D_{s,x}$ or $D_{s,y}$ goes to zero. Using BKT theory we can show that

$$k_B T_c = \frac{\pi}{2} (D_{s,x}(T_c^-) D_{s,y}(T_c^-))^{1/2} \quad (\text{H3})$$

which leads to the improved bound

$$k_B T_c \leq \frac{\pi}{2} \left(\tilde{D}_x \tilde{D}_y \right)^{1/2} \quad (\text{H4})$$

To derive equation (H3) we start with the Free energy for phase fluctuations

$$\mathcal{F} = \frac{1}{2} \int dx dy [D_{s,x}(\partial_x \theta)^2 + D_{s,y}(\partial_y \theta)^2]. \quad (\text{H5})$$

We then rescale lengths using $x' = (D_0/D_{s,x})^{1/2}x$ and $y' = (D_0/D_{s,y})^{1/2}y$, where D_0 is any convenient energy scale for normalization, to obtain

$$\mathcal{F} = \frac{1}{2} (D_{s,x} D_{s,y})^{1/2} \int dx' dy' [(\partial_{x'} \theta)^2 + (\partial_{y'} \theta)^2]. \quad (\text{H6})$$

This immediately leads to the generalization of the Nelson-Kosterlitz result in equation (H3). We emphasize that the reason this seemingly naive argument works is that the line of fixed points below T_c are actually described by a Gaussian theory and the BKT T_c is precisely when vortex-antivortex unbinding becomes relevant at a Gaussian fixed point. We thank Steve Kivelson and C. Jayaprakash for very useful conversations related to this argument.